

Supporting Information for:

Evaluating Metal-Organic Frameworks for Post-Combustion Carbon Dioxide Capture via Temperature Swing Adsorption

*Jarad A. Mason,^a Kenji Sumida,^a Zoey R. Herm,^a Rajamani Krishna,^{*b} Jeffrey R. Long^{*a}*

^a Department of Chemistry, University of California, Berkeley and Materials Sciences Division, Lawrence Berkeley National Laboratory, Berkeley, CA 94720, USA. E-mail: jrlong@berkeley.edu

^bVan't Hoff Institute for Molecular Sciences, University of Amsterdam, Science Park 904, 1098 XH Amsterdam, The Netherlands. E-mail: r.krishna@uva.nl

Energy Environ. Sci.

List of Contents

1. Experimental characterization	S-3
2. High-pressure CO ₂ data.....	S-6
3. Heat capacity of MOF-177 and Mg ₂ (dobdc) under He.....	S-6
4. Fitting of isotherms.....	S-7
5. Single-site Langmuir model for adsorption isotherms.....	S-7
6. Dual-site Langmuir model for CO ₂ adsorption isotherm	S-9
7. Q_{st} determination for dual-site Langmuir isotherm.....	S-10
8. Isotherm fits for zeolite NaX.....	S-13
9. Notation	S-13
10. Parameters for isotherm fits.....	S-13
Figures	S-19
References.....	S-27

1. Experimental Characterization

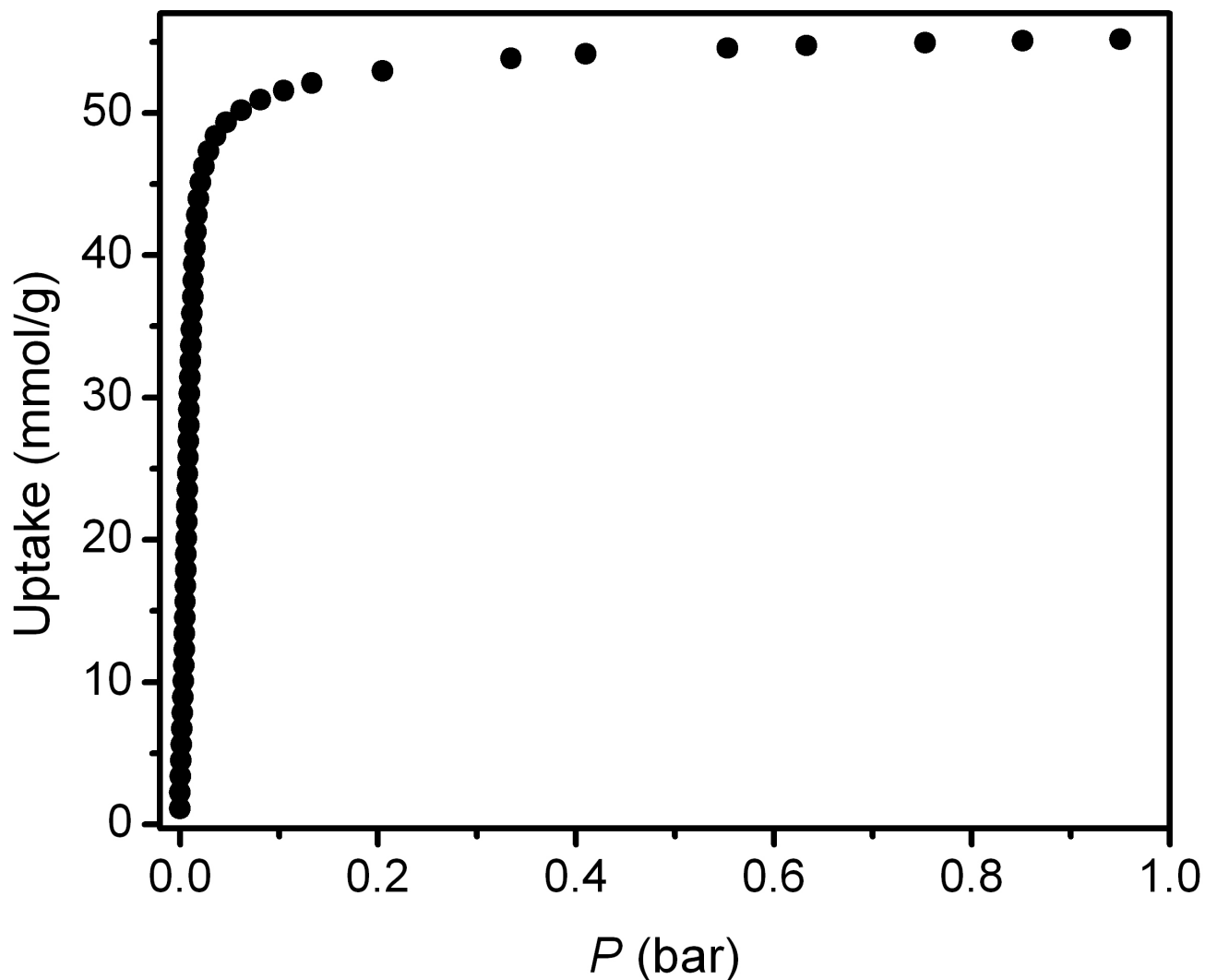


Fig. S1. Adsorption isotherm for N₂ in MOF-177 at 77 K, resulting in a calculated Langmuir surface area of 5400 m²/g and BET surface area of 4690 m²/g.

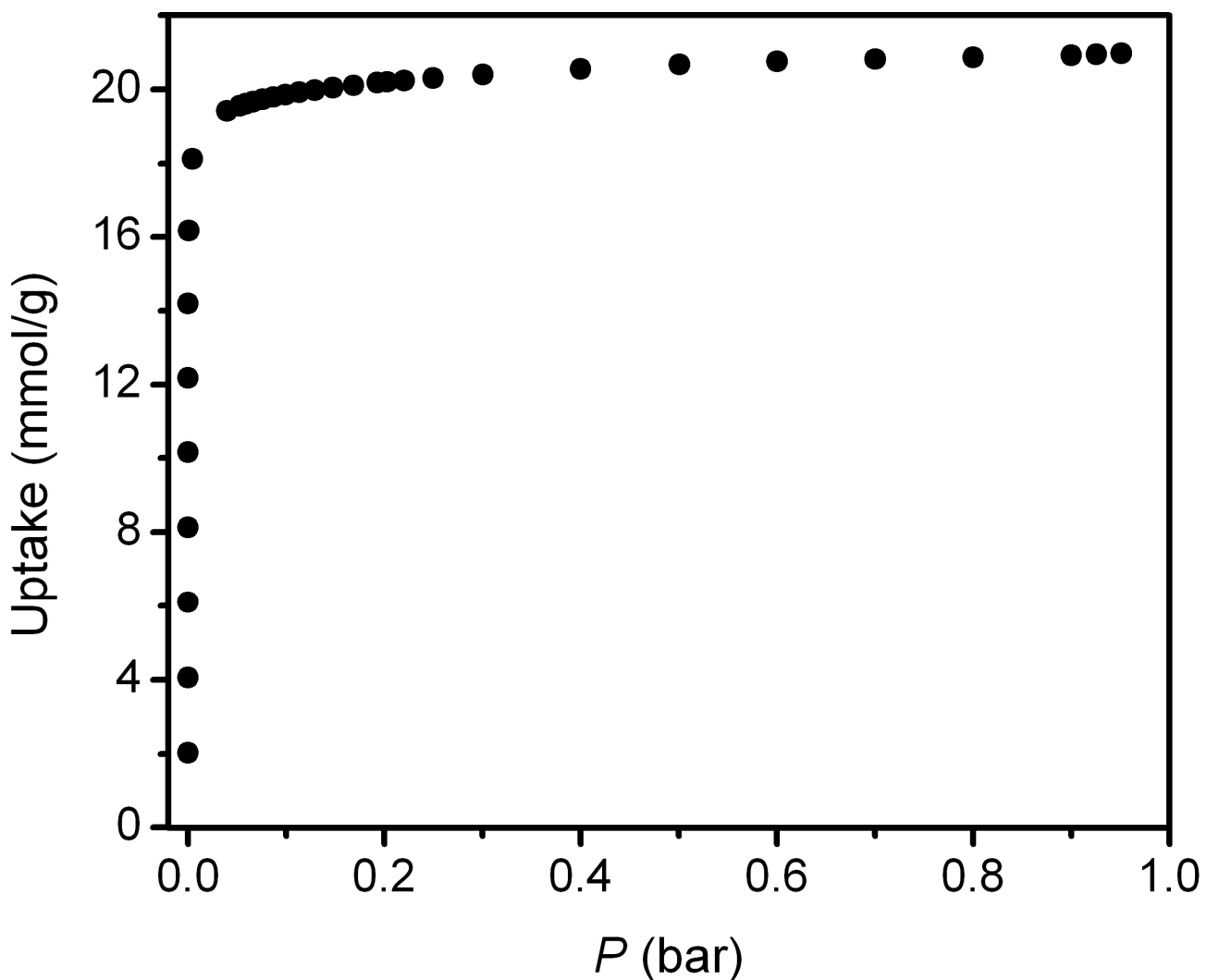


Fig. S2. Adsorption isotherm for N_2 in $\text{Mg}_2(\text{dodbc})$ at 77 K, resulting in a calculated Langmuir surface area of $2060 \text{ m}^2/\text{g}$ and BET surface area of $1800 \text{ m}^2/\text{g}$.

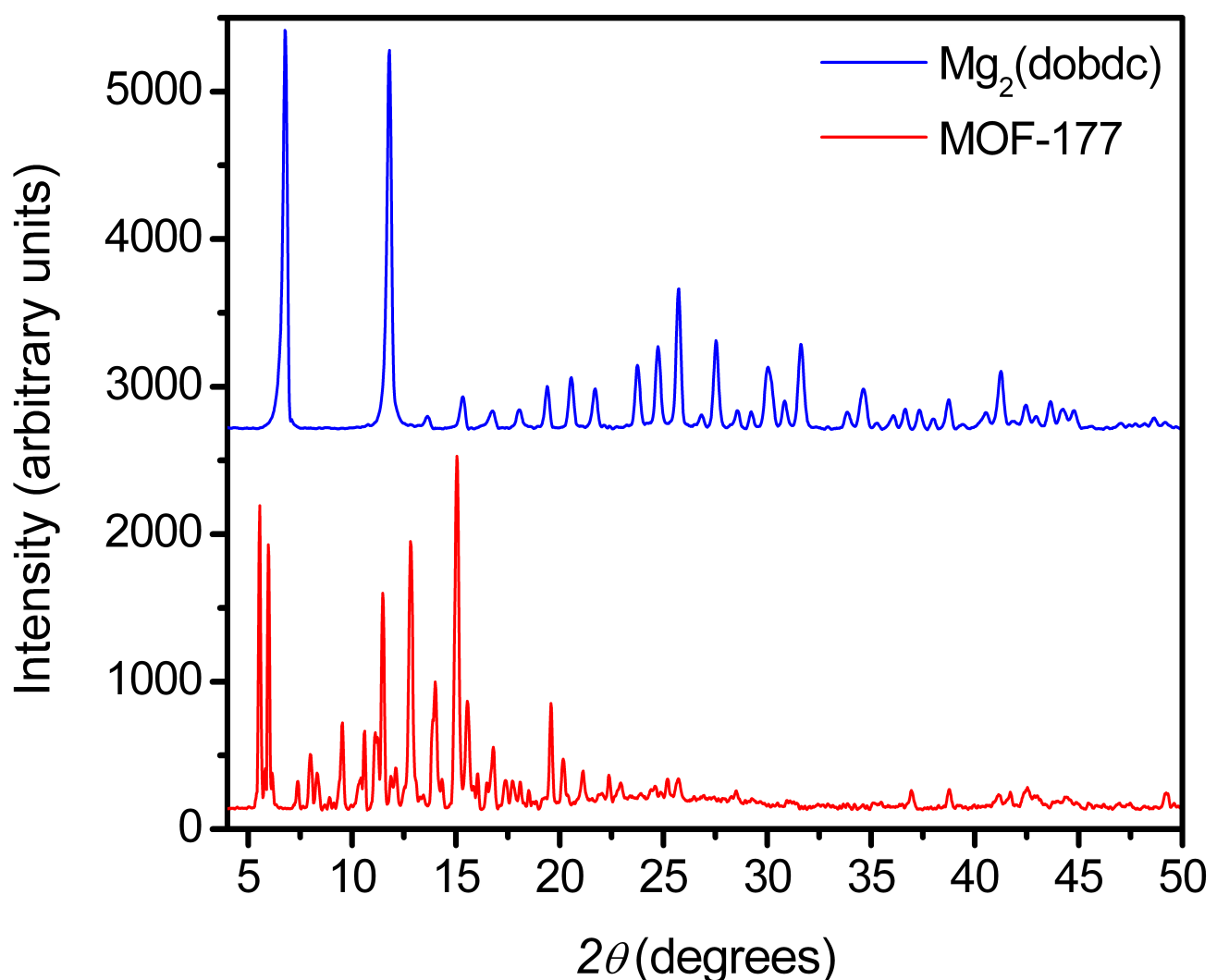


Fig. S3. X-ray powder diffraction patterns, with background subtracted, of as synthesized MOF-177 (bottom) and $\text{Mg}_2(\text{dobdc})$ (top).

2. High-Pressure CO₂ Data

Table S1. High-pressure CO₂ adsorption data for Mg₂(dobdc) at 50 °C. The high-pressure CO₂ adsorption data for MOF-177 and Mg₂(dobdc) at 40 °C was previously reported.¹

Pressure (bar)	Excess Uptake (mmol/g)	Total Uptake (mmol/g)
2.4585	8.65423	8.708273358
7.967838	11.47412	11.65650558
14.34587	12.83591	13.17339535
21.16477	13.32603	13.84033891
28.33638	13.35482	14.0713281
35.79211	13.1753	14.12419199
43.65606	12.37505	13.59879711
50.21045	10.71721	12.19738362

3. Heat Capacity of MOF-177 and Mg₂(dobdc) under He

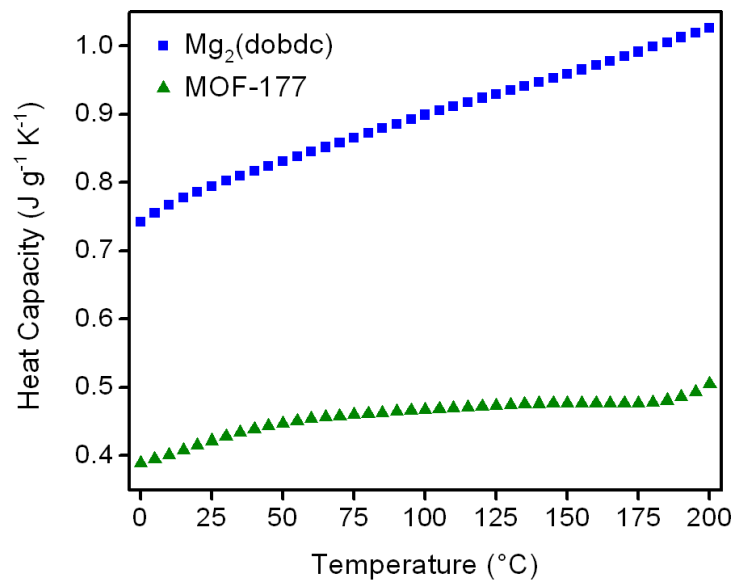


Fig. S4. Heat capacity of MOF-177 (green triangles) and Mg₂(dobdc) (blue squares) as a function of temperature measured under He.

4. Fitting of isotherms

The measured experimental data on pure component isotherms for CO₂ and N₂, in terms of excess loadings, in MOF-177 and Mg₂(dobdc) at temperatures ranging from 293 K to 473 K were first converted to absolute loading using the Peng-Robinson equation of state for estimation of the fluid densities. For calculation of the absolute component loadings, the pore volume data of Herm et al.¹ was used. For MOF-177 and Mg₂(dobdc), the pore volumes are 1.59 cm³/g and 0.573 cm³/g, respectively.

The absolute component loadings were fitted with either a single-site Langmuir model or a dual-site Langmuir model, as discussed below.

5. Single-site Langmuir model for adsorption isotherms

For CO₂/MOF-177, N₂/MOF-177, and N₂/Mg₂(dobdc) there are no discernible isotherm inflections and therefore the single-site Langmuir model

$$q = \frac{q_{sat}bp}{1+bp} \quad (1)$$

was used for isotherm fitting for these three guest/host combinations. The temperature dependence of the Langmuir constant, *b*, is expressed as

$$b = b_0 \exp\left(\frac{E}{RT}\right); \quad \ln(b) = \ln(b_0) + \frac{E}{RT} \quad (2)$$

Equation (1) can be expressed in terms of the fractional occupancy, θ , as follows

$$\theta \equiv \frac{q}{q_{sat}} = \frac{bp}{1+bp} \quad (3)$$

Re-arranging equation (3) yields

$$p = \frac{1}{b} \frac{1}{1-\theta} \quad (4)$$

and

$$\ln p = -\ln(b) - \ln(1-\theta) \quad (5)$$

The isosteric heat of adsorption, Q_{st} , is defined as

$$Q_{st} = RT^2 \left(\frac{\partial \ln p}{\partial T} \right)_q \quad (6)$$

where the derivative in the right member of equation (6) is determined at constant adsorbate loading, q .

Using equation (6) we can write the following expression for the isosteric heat of adsorption in which the derivative with respect to temperature is at constant occupancy \square

$$Q_{st} = RT^2 \left(\frac{\partial \ln p}{\partial T} \right)_\theta = -RT^2 \left(\frac{\partial \ln b}{\partial T} \right)_\theta \quad (7)$$

Differentiating equation (2) yields

$$Q_{st} = -E \quad (8)$$

Fig. S5 shows the experimental data for adsorption of CO₂ in MOF-177 at a variety of temperatures. The continuous solid lines are the single-site Langmuir fits using the parameters specified in Table S2.

Fig. S6 shows the experimental data for adsorption of N₂ in MOF-177 at a variety of temperatures. The continuous solid lines are the single-site Langmuir fits using the parameters specified in Table S3.

Fig. S7 shows the experimental data for adsorption of N₂ in Mg₂(dobdc) at a variety of temperatures. The continuous solid lines are the single-site Langmuir fits using the parameters specified in Table S4.

The parity plots in Fig. S5e, S6e, and S7e indicate that the fits are good over the entire range of loadings.

Fig. S8 presents a comparison of the isosteric heats of adsorption, Q_{st} , for CO₂/MOF-177, N₂/MOF-177, and N₂/Mg₂(dobdc). For all three guest/host combinations Q_{st} is independent of the adsorbate loading.

The situation with CO₂/Mg₂(dobdc) is different and a similar approach to the above using single-site Langmuir model fits is inadequate. This is demonstrated in Fig. S9 which shows the parity plot for fitting the experimental data, all of which were measured for pressure up to 100 kPa, to a single-site Langmuir model. The statistical “best” fit yields significant deviations at either ends of the loading

range; see the parity plots in Fig. S9 comparing the experimental values of absolute loadings for CO₂/Mg₂(dobdc) measured in this work and the values of the loadings calculated using the single-site Langmuir model along with the parameters specified in Table S5 (y-axis). The important conclusion to be drawn here is that even though the experimental loadings are below 8 mol/kg, the single-site Langmuir model provides an inadequate description for the entire range of temperatures. Below we show that the dual-site Langmuir model provides a good description of the dataset.

6. Dual-site Langmuir model for CO₂ adsorption isotherm

Fig. S10 presents the adsorption isotherms for CO₂ in Mg₂(dobdc) at 278 K, 298 K, 343 K, 393 K, and 473 K measured in the work of Dietzel et al.² The isotherms at 278 K, 298 K, 343 K, show a clear inflection at a loading of 1 molecule CO₂ adsorbed per Mg atom, corresponding to about 8 mol/kg.

Fig. S11 shows the adsorption isotherms for CO₂ in Mg₂(dobdc) at 313 K measured in the work of Herm et al.¹ The inflection characteristic at a loading of 8 mol/kg is again clearly evident.

The inflection characteristics necessitates the use of the dual-site Langmuir model

$$q \equiv q_A + q_B = \frac{q_{sat,A} b_A p}{1 + b_A p} + \frac{q_{sat,B} b_B p}{1 + b_B p} \quad (9)$$

where we have two distinct adsorption sites A and B. Table S6 provides the fit constants. In this fitting procedure, the entire set of isotherm data measured in the current work, along with those of Dietzel et al.² and Herm et al.¹ were used. The continuous solid lines in Fig. S10 and S11 represent calculations of the absolute CO₂ loadings using equation (9), along with the parameters specified in Table S6. For both sets of experimental data, the dual-site Langmuir model provides a good description of the inflection characteristics.

Fig. S12 presents a comparison of the experimentally measured absolute loadings of CO₂ for temperatures ranging from 293 K to 473 K with calculations of the absolute CO₂ loadings using equation (9), along with the parameters specified in Table S6. The agreement is good for the entire dataset.

The next question we address is the determination of the isosteric heat of adsorption, Q_{st} , using equation (6). For carrying out the analytic differentiation we need to express the pressure explicitly in terms of the loading.

7. Q_{st} determination for dual-site Langmuir isotherm

We can rewrite equation (9) as a quadratic polynomial of the pressures:

$$(q_{sat,A} + q_{sat,B} - q)b_A b_B p^2 + ((q_{sat,A} - q)b_A + (q_{sat,B} - q)b_B)p - q = 0 \quad (10)$$

In proceeding further it is convenient to define the following two parameters α and β

$$\alpha = (q_{sat,A} + q_{sat,B} - q)b_A b_B \quad (11)$$

and

$$\beta = (q_{sat,A} - q)b_A + (q_{sat,B} - q)b_B \quad (12)$$

For any specified loading q , the corresponding pressure is obtained by solving the quadratic equation (10), yielding

$$p = \frac{-\beta \pm \sqrt{\beta^2 + 4\alpha q}}{2\alpha} \quad (13)$$

Only one of the two solutions in equation (13) is physically realizable; this is given by:

$$p = \frac{-\beta + \sqrt{\beta^2 + 4\alpha q}}{2\alpha} = \frac{\sqrt{\beta + 4\alpha q} - \beta}{2\alpha} \quad (14)$$

The logarithm of the pressure is therefore

$$\ln p = \ln(\sqrt{\beta + 4\alpha q} - \beta) - \ln 2\alpha \quad (15)$$

The derivative $\left(\frac{\partial \ln p}{\partial T} \right)_q$, keeping the loading constant, can be derived as follows.

$$\frac{\partial \ln p}{\partial T} = \frac{\partial \ln(\sqrt{\beta + 4\alpha q} - \beta)}{\partial T} - \frac{\partial \ln 2\alpha}{\partial T} \quad (16)$$

$$\frac{\partial \ln p}{\partial T} = \frac{1}{(\sqrt{\beta + 4\alpha q} - \beta)} \frac{\partial (\sqrt{\beta + 4\alpha q} - \beta)}{\partial T} - \frac{1}{2\alpha} \frac{\partial 2\alpha}{\partial T} \quad (17)$$

$$\frac{\partial \ln p}{\partial T} = \frac{1}{(\sqrt{\beta + 4\alpha q} - \beta)} \left(\frac{\partial (\sqrt{\beta + 4\alpha q})}{\partial T} - \frac{\partial \beta}{\partial T} \right) - \frac{1}{\alpha} \frac{\partial \alpha}{\partial T} \quad (18)$$

$$\frac{\partial \ln p}{\partial T} = \frac{1}{(\sqrt{\beta + 4\alpha q} - \beta)} \left(\frac{1}{2\sqrt{\beta^2 + 4\alpha q}} \frac{\partial (\beta^2 + 4\alpha q)}{\partial T} - \frac{\partial \beta}{\partial T} \right) - \frac{1}{\alpha} \frac{\partial \alpha}{\partial T} \quad (19)$$

$$\frac{\partial \ln p}{\partial T} = \frac{1}{(\sqrt{\beta^2 + 4\alpha q} - \beta)} \left(\frac{1}{2\sqrt{\beta^2 + 4\alpha q}} \left(\frac{\partial \beta^2}{\partial T} + 4q \frac{\partial \alpha}{\partial T} \right) - \frac{\partial \beta}{\partial T} \right) - \frac{1}{\alpha} \frac{\partial \alpha}{\partial T} \quad (20)$$

$$\frac{\partial \ln p}{\partial T} = \frac{1}{(\sqrt{\beta^2 + 4\alpha q} - \beta)} \left(\frac{1}{2\sqrt{\beta^2 + 4\alpha q}} \left(2\beta \frac{\partial \beta}{\partial T} + 4q \frac{\partial \alpha}{\partial T} \right) - \frac{\partial \beta}{\partial T} \right) - \frac{1}{\alpha} \frac{\partial \alpha}{\partial T} \quad (21)$$

The derivatives of α and β with respective to temperature at constant loading q can be obtained as follows

$$\frac{\partial \alpha}{\partial T} = (q_{sat,A} + q_{sat,B} - q) \frac{\partial (b_A b_B)}{\partial T} \quad (22)$$

$$\frac{\partial \beta}{\partial T} = (q_{sat,A} - q) \frac{\partial (b_A)}{\partial T} + (q_{sat,B} - q) \frac{\partial (b_B)}{\partial T} \quad (23)$$

If the temperature dependence of the two Langmuir constants b_A and b_B are described by

$$b_A = b_{A0} \exp\left(\frac{E_A}{RT}\right); \quad b_B = b_{B0} \exp\left(\frac{E_B}{RT}\right) \quad (24)$$

we can derive the following set of relations

$$\frac{\partial b_A}{\partial T} = -b_{A0} \exp\left(\frac{E_A}{T}\right) \frac{E_A}{RT^2}; \quad \frac{\partial b_B}{\partial T} = -b_{B0} \exp\left(\frac{E_B}{T}\right) \frac{E_B}{T^2} \quad (25)$$

$$b_A b_B = b_{A0} b_{B0} \exp\left(\frac{E_A + E_B}{RT}\right) \quad (26)$$

$$\frac{\partial(b_A b_B)}{\partial T} = -b_{A0} b_{B0} \exp\left(\frac{E_A + E_B}{RT}\right) \frac{E_A + E_B}{RT^2} \quad (27)$$

Combining equations (21), (22), (23), (25), and (27) with equation (6) allows the explicit determination of the isosteric heat of adsorption Q_{st} . The calculation of the isosteric heat of adsorption for CO₂/Mg₂(dobdc), using the analytic procedure developed above is given in Fig. S13a. The value of Q_{st} varies from 42 kJ mol⁻¹ at low loadings to 24 kJ mol⁻¹ at high loading. The Q_{st} values are only weakly dependent on temperature.

Fig. S13b presents a comparison of our Q_{st} with the published data of Dietzel et al.² and Simmons et al.³ All three datasets demonstrate the strong inflection characteristics of Q_{st} . The Q_{st} calculations of Dietzel et al.² and Simmons et al.³ for loadings higher than 8 mol/kg show an increase in Q_{st} that is not reflected in our calculations. This increase is most likely caused due to the fact that in the calculations of Dietzel et al.² and Simmons et al.³ the adsorbed phase loadings were not converted from excess to absolute values; the differences in these two loadings is not negligible at high pressures.

In the recent paper by Bao et al.,⁴ experimental data on CO₂ adsorption in Mg₂(dobdc) has been presented for temperatures of 278 K, 298 K, and 318 K. Figure S14 provides a comparison of their experimental isotherms with calculations of the absolute loading using the dual-Langmuir fits with parameters specified in Table S6. It is noted that the agreement between the two sets is very good. This agreement also implies that their experimental data should yield isosteric heats of adsorption that are the same as those presented in Figure S13a. Curiously, the calculations of the isosteric heats of adsorption presented in Figure 8 of Bao et al.⁴ are significantly higher. Their values range from 73 kJ/mol at low adsorption loadings to 45 kJ/mol at a loading of 2.6 mol/kg. It appears that their calculations of the isosteric heats of adsorption are not correct; their Q_{st} calculations are clearly inconsistent with their experimental isotherm data.

8. Isotherm fits for zeolite NaX

For comparing the performance of Mg₂(dobdc) with zeolite NaX in post combustion carbon capture we used the experimental data of Belmabkhout et al.⁵ and Cavenati et al.⁶ for adsorption of CO₂ and N₂ at a variety of temperatures. The dual-site Langmuir model was used for fitting purposes. The fitted parameters are specified in Tables S7 and S8.

9. Notation

<i>b</i>	parameter in the pure component Langmuir adsorption isotherm, Pa ⁻¹
- <i>E</i>	heat of adsorption, J mol ⁻¹
<i>p</i>	bulk gas phase pressure, Pa
<i>q</i>	molar loading of adsorbate, mol kg ⁻¹
<i>q</i> _{sat}	saturation loading, mol kg ⁻¹
<i>Q</i> _{st}	isosteric heat of adsorption, J mol ⁻¹
<i>R</i>	gas constant, 8.314 J mol ⁻¹ K ⁻¹
<i>T</i>	absolute temperature, K

Greek letters

\square	parameter defined by equation (11), mol kg ⁻¹ Pa ⁻¹
\square	parameter defined by equation (12), mol kg ⁻¹ Pa ⁻¹
\square	fractional occupancy, dimensionless

Subscripts

A	referring to site A
B	referring to site A
sat	referring to saturation conditions

10. Parameters for Isotherm Fits

Table S2. Single-site Langmuir parameter for adsorption of CO₂ in MOF-177. These parameters were determined by fitting adsorption isotherms for temperatures ranging from 293 K to 473 K.

$$q = \frac{q_{sat}bp}{1+bp}$$

$$q_{sat} = 48 \text{ mol kg}^{-1}$$

$$b = b_0 \exp\left(\frac{E}{RT}\right);$$

$$b_0 = 8.06 \times 10^{-10} \text{ Pa}^{-1}$$

$$E = 14 \text{ kJ mol}^{-1}$$

Table S3. Single-site Langmuir parameter for adsorption of N₂ in MOF-177. These parameters were determined by fitting adsorption isotherms for temperatures ranging from 293 K to 473 K.

$$q = \frac{q_{sat}bp}{1+bp}$$

$$q_{sat} = 48 \text{ mol kg}^{-1}$$

$$b = b_0 \exp\left(\frac{E}{RT}\right);$$

$$b_0 = 1.11 \times 10^{-9} \text{ Pa}^{-1}$$

$$E = 10 \text{ kJ mol}^{-1}$$

Table S4. Single-site Langmuir parameter for adsorption of N₂ in Mg₂(dobdc). These parameters were determined by fitting adsorption isotherms for temperatures ranging from 293 K to 473 K.

$$q = \frac{q_{sat}bp}{1+bp}$$

$$q_{sat} = 14 \text{ mol kg}^{-1}$$

$$b = b_0 \exp\left(\frac{E}{RT}\right);$$

$$b_0 = 4.96 \times 10^{-10} \text{ Pa}^{-1}$$

$$E = 18 \text{ kJ mol}^{-1}$$

Table S5. Single-site Langmuir parameter for adsorption of CO₂ in Mg₂(dobdc). These parameters were determined by fitting adsorption isotherms for temperatures ranging from 293 K to 473 K. The choice of $E = 42 \text{ kJ/mol}$ is dictated by the fact that the measured data have loadings in the range 0 – 8 mol/kg and in this range the isosteric heat of adsorption is 42 kJ/mol as reported in the work of Dietzel et al.²

$$q = \frac{q_{sat}bp}{1+bp}$$

$$q_{sat} = 7.9 \text{ mol kg}^{-1}$$

$$b = b_0 \exp\left(\frac{E}{RT}\right);$$

$$b_0 = 1.557 \times 10^{-11} \text{ Pa}^{-1}$$

$$E = 42 \text{ kJ mol}^{-1}$$

Table S6. Dual-site Langmuir parameter for adsorption of CO₂ in Mg₂(dobdc). These parameters were determined by fitting adsorption isotherms for temperatures ranging from 278 K to 473 K.

$$q \equiv q_A + q_B = \frac{q_{sat,A} b_A p}{1 + b_A p} + \frac{q_{sat,B} b_B p}{1 + b_B p}$$

$$q_{sat,A} = 6.8 \text{ mol kg}^{-1}$$

$$q_{sat,B} = 9.9 \text{ mol kg}^{-1}$$

$$b_A = b_{A0} \exp\left(\frac{E_A}{RT}\right);$$

$$b_{A0} = 2.44 \times 10^{-11} \text{ Pa}^{-1}$$

$$E_A = 42 \text{ kJ mol}^{-1}$$

$$b_B = b_{B0} \exp\left(\frac{E_B}{RT}\right);$$

$$b_{B0} = 1.39 \times 10^{-10} \text{ Pa}^{-1}$$

$$E_B = 24 \text{ kJ mol}^{-1}$$

Table S7. Dual-site Langmuir parameter for adsorption of CO₂ in NaX zeolite. These parameters were determined by fitting adsorption isotherm data reported in the works of Belmabkhout et al.⁵ and Cavenati et al.⁶

$$q \equiv q_A + q_B = \frac{q_{sat,A} b_A p}{1 + b_A p} + \frac{q_{sat,B} b_B p}{1 + b_B p}$$

$$q_{sat,A} = 3.5 \text{ mol kg}^{-1}$$

$$q_{sat,B} = 5.2 \text{ mol kg}^{-1}$$

$$b_A = b_{A0} \exp\left(\frac{E_A}{RT}\right);$$

$$b_{A0} = 3.64 \times 10^{-13} \text{ Pa}^{-1}$$

$$E_A = 35 \text{ kJ mol}^{-1}$$

$$b_B = b_{B0} \exp\left(\frac{E_B}{RT}\right);$$

$$b_{B0} = 6.04 \times 10^{-11} \text{ Pa}^{-1}$$

$$E_B = 35 \text{ kJ mol}^{-1}$$

Table S8. Dual-site Langmuir parameter for adsorption of N₂ in Zeolite NaX. These parameters were determined by fitting adsorption isotherm data reported in the works of Belmabkhout et al.⁴ and Cavenati et al.⁵

$$q \equiv q_A + q_B = \frac{q_{sat,A} b_A p}{1 + b_A p} + \frac{q_{sat,B} b_B p}{1 + b_B p}$$

$$q_{sat,A} = 3 \text{ mol kg}^{-1}$$

$$q_{sat,B} = 6 \text{ mol kg}^{-1}$$

$$b_A = b_{A0} \exp\left(\frac{E_A}{RT}\right);$$

$$b_{A0} = 4.08 \times 10^{-9} \text{ Pa}^{-1}$$

$$E_A = 13 \text{ kJ mol}^{-1}$$

$$b_B = b_{B0} \exp\left(\frac{E_B}{RT}\right);$$

$$b_{B0} = 4.68 \times 10^{-10} \text{ Pa}^{-1}$$

$$E_B = 13 \text{ kJ mol}^{-1}$$

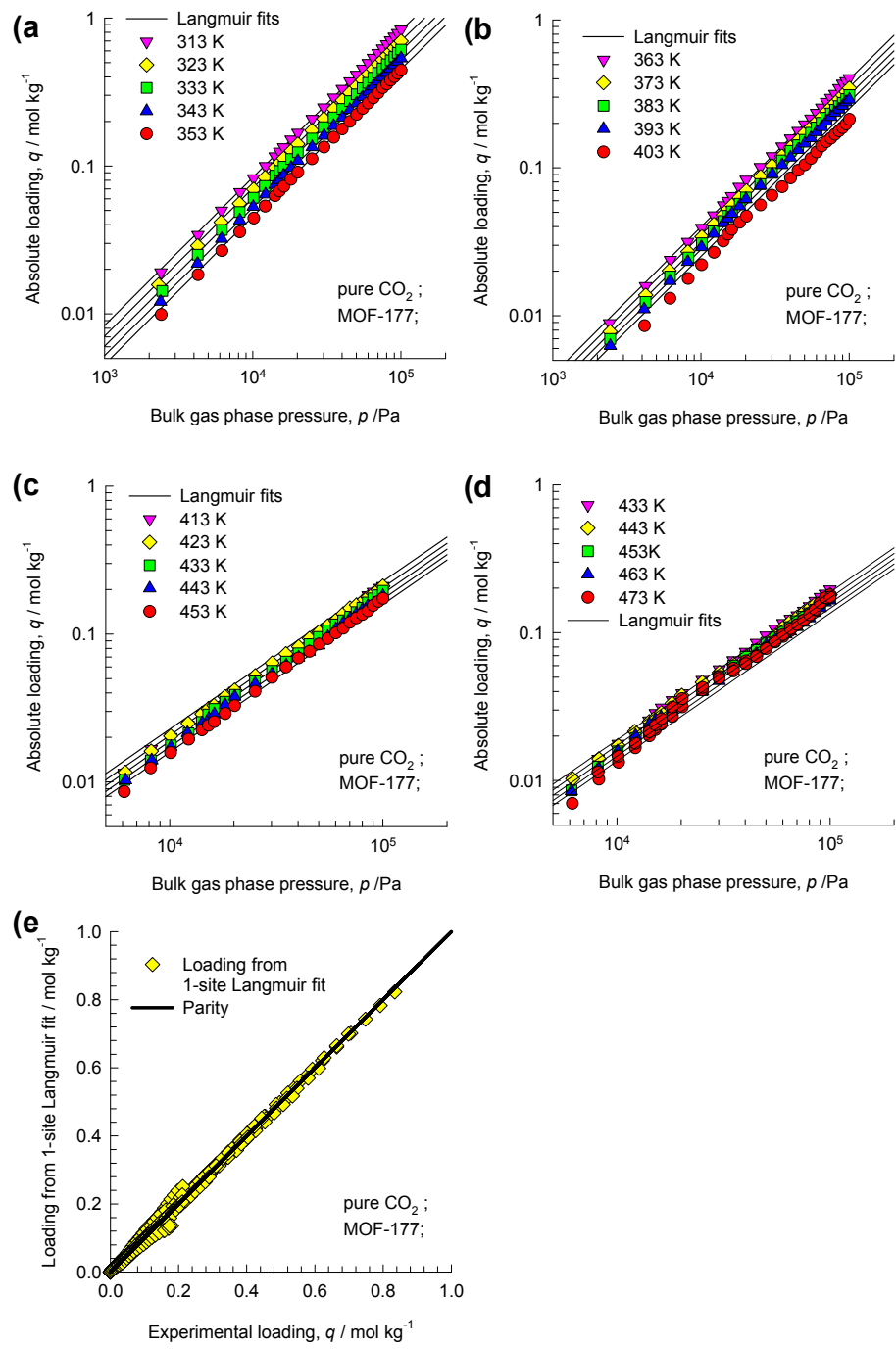


Fig. S5. (a, b, c, d) Experimental data for adsorption of CO_2 in MOF-177. The continuous solid lines are the single-site Langmuir fits using the parameters specified in Table S2. (e) Parity plot comparing the experimentally measured absolute loadings for the entire data set (x-axis) and the values of the loadings calculated using the single-site Langmuir model along with the parameters specified in Table S2 (y-axis).

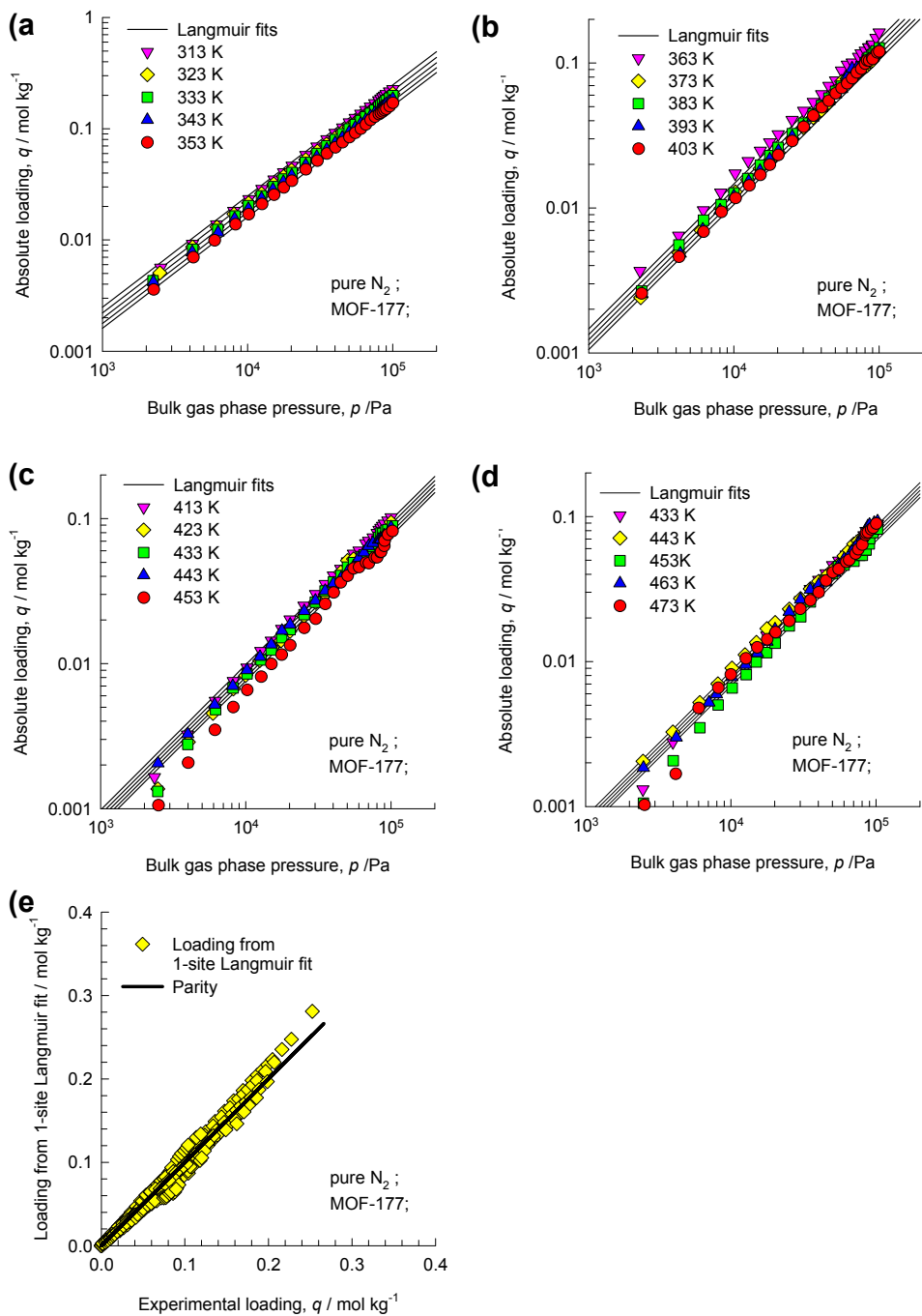


Fig. S6. (a, b, c, d) Experimental data for adsorption of N_2 in MOF-177. The continuous solid lines are the single-site Langmuir fits using the parameters specified in Table S3. (e) Parity plot comparing the experimentally measured absolute loadings for the entire dataset (x -axis) and the values of the loadings calculated using the single-site Langmuir model along with the parameters specified in Table S3 (y -axis).

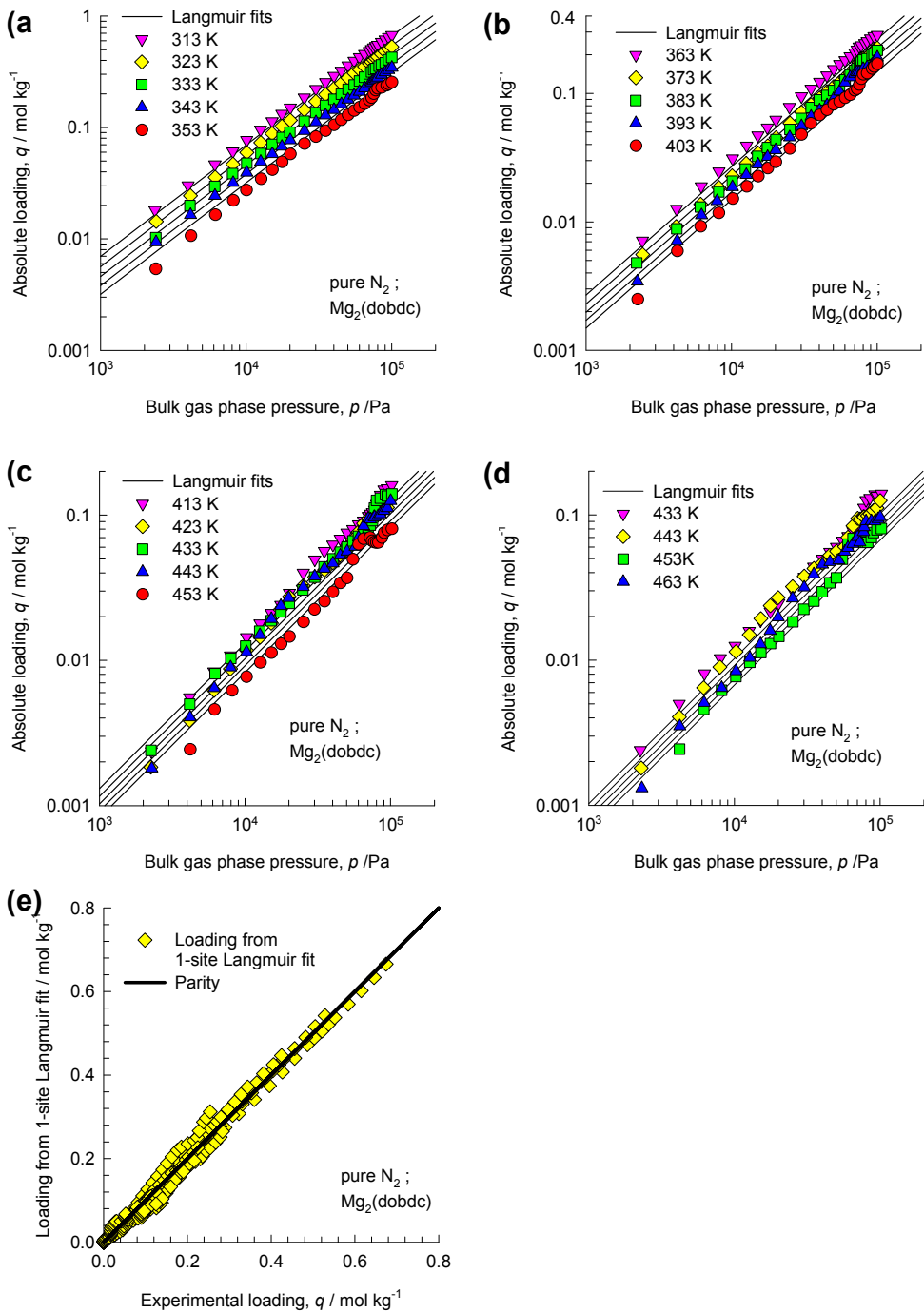


Fig. S7. (a, b, c, d) Experimental data for adsorption of N_2 in $\text{Mg}_2(\text{dobdc})$. The continuous solid lines are the single-site Langmuir fits using the parameters specified in Table S4. (e) Parity plot comparing the experimentally measured absolute loadings for the entire data set (x -axis) and the values of the loadings calculated using the single-site Langmuir model along with the parameters specified in Table S4 (y -axis).

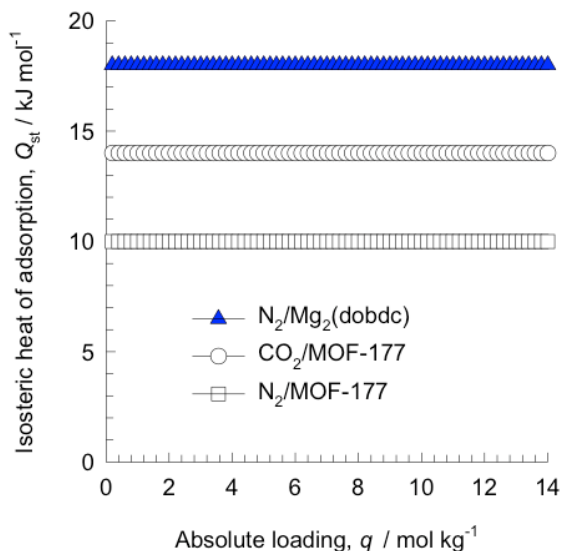


Fig. S8. Comparison of the isosteric heats of adsorption, Q_{st} , for $CO_2/\text{MOF-177}$, $N_2/\text{MOF-177}$, and $N_2/Mg_2(\text{dobdc})$.

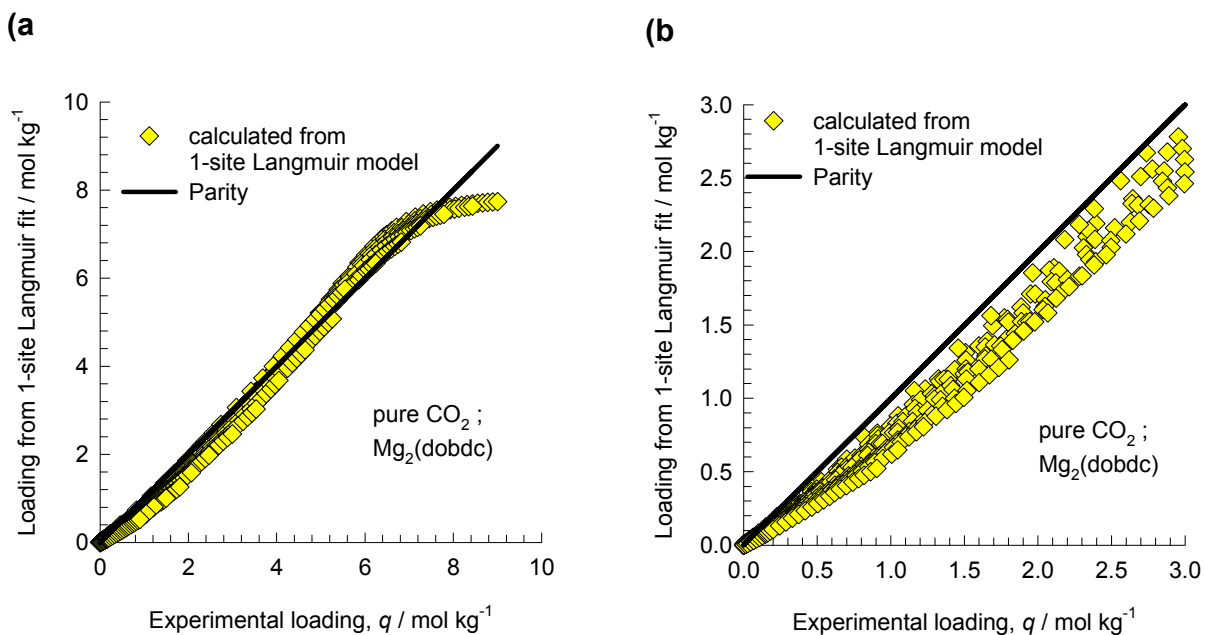


Fig. S9. Parity plot comparing the experimental values of absolute loadings for $CO_2/\text{Mg}_2(\text{dobdc})$ measured in this work and the values of the loadings calculated using the single-site Langmuir model along with the parameters specified in Table S5 (y -axis).

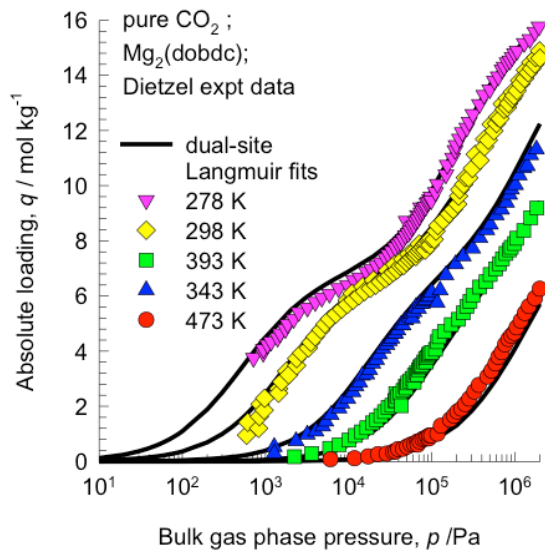


Fig. S10. Adsorption isotherms for CO₂ in Mg₂(dobdc) at 278 K, 298 K, 343 K, 393 K, and 473 K measured in the work of Dietzel et al.². Their data for excess loadings have been converted to absolute loadings by estimating the fluid densities within the pores using the Peng-Robinson equation of state. Their experimental value of the pore volume, 0.63 cm³/g, was used in this conversion. The continuous solid lines are the dual-site Langmuir fits using the parameters specified in Table S6.

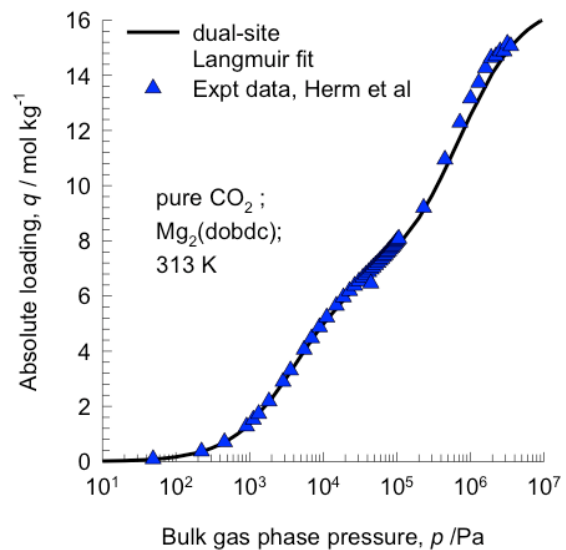


Fig. S11. Adsorption isotherms for CO₂ in Mg₂(dobdc) at 313 K measured in the work of Herm et al.¹

The continuous solid lines are the dual-site Langmuir fits using the parameters specified in Table S6.

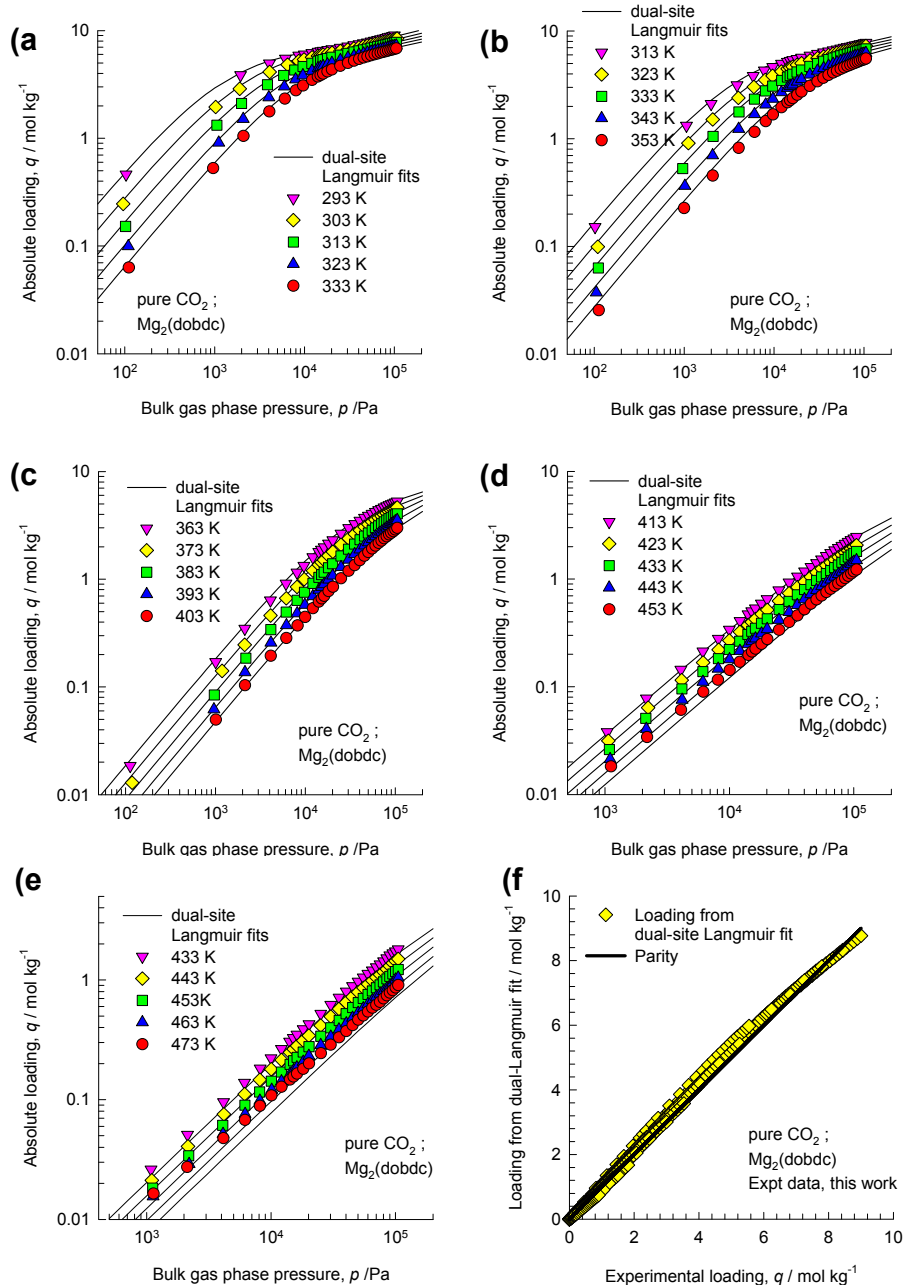


Fig. S12. (a, b, c, d, e) Experimental data for adsorption of CO₂ in Mg₂(dobdc) for a variety of temperatures generated in the current work. The continuous solid lines are the dual-site Langmuir fits using the parameters specified in Table S6. (f) Parity plot comparing the experimentally measured absolute loadings for the entire data set (x -axis) and the values of the loadings calculated using the dual-site Langmuir model along with parameters specified in Table S6 (y -axis). The parity plot includes only the dataset generated in this work.

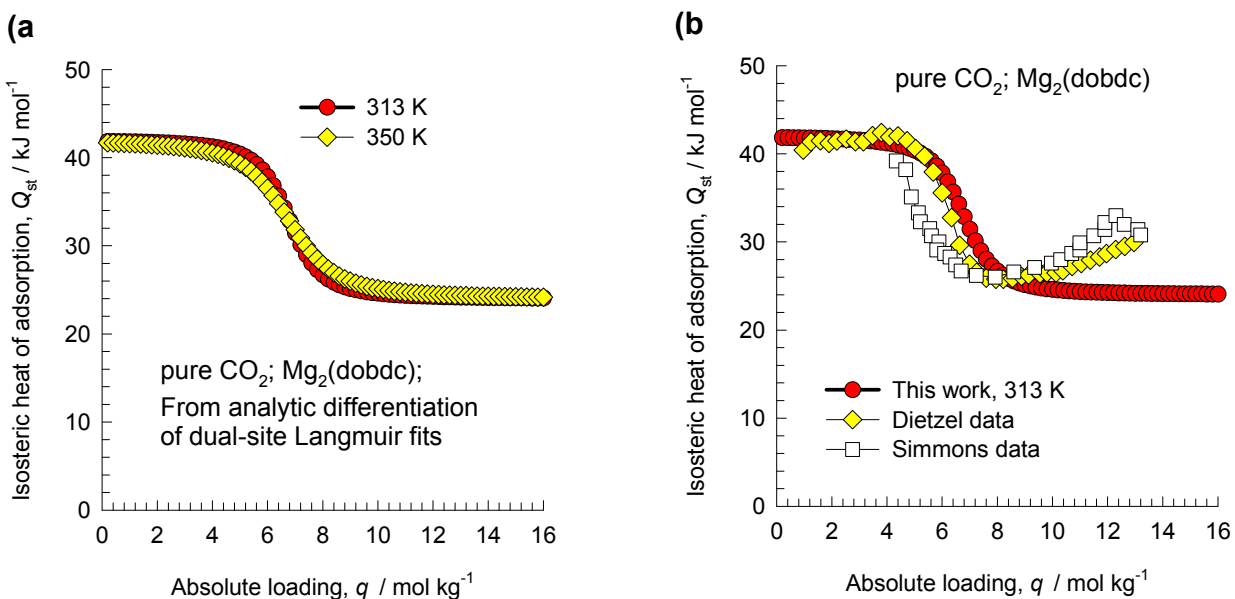


Fig. S13. (a) The isosteric heats of adsorption, Q_{st} , for $\text{CO}_2/\text{Mg}_2(\text{dobdc})$ obtained from analytic differentiation of the dual-site Langmuir fits. The Q_{st} are shown for 313 K and 350 K. We note that the temperature dependence is very weak. (b) Comparison of our Q_{st} with the published data of Dietzel et al.² and Simmons et al.³

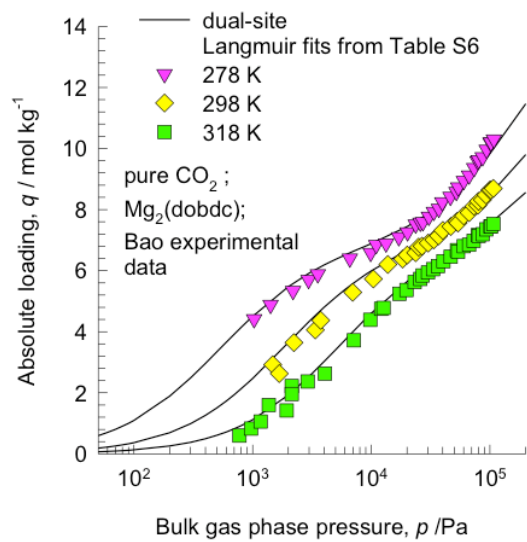


Fig. S14. Experimental data of Bao et al.⁴ (denoted by symbols) of CO_2 isotherms in $\text{Mg}_2(\text{dobdc})$ at 278 K, 298 K, and 318 K, compared with calculations of the absolute loading using the dual-Langmuir fits with parameters specified in Table S6.

References

- (1) Z. H. Herm, J. A. Swisher, B. Smit, R. Krishna and J. R. Long, *J. Am. Chem. Soc.*, 2011, **133**, 5664.
- (2) P. D. C. Dietzel, V. Besikiotis and R. Blom, *J. Mater. Chem.*, 2009, **19**, 7362.
- (3) J. M. Simmons, H. Wu, W. Zhou and T. Yildirim, *Energy Environ. Sci.*, 2011, **4**, 2177.
- (4) Z. Bao, L. Yu, Q. Ren, X. Lu and S. Deng, *J. Colloid Interface Sci.*, 2011, **353**, 549.
- (5) Y. Belmabkhout, G. Pirngruber, E. Jolimaitre, A. Methivier, *Adsorption*, 2007, **13**, 341.
- (6) S. Cavenati, C. A. Grande and A. E. Rodrigues, *J. Chem. Eng. Data*, 2004, **49**, 1095.